

# Distinct Element Simulations of Granular Shear Zones: Micromechanics of Localization and Frictional Behavior

Julia K. Morgan

Department of Geology and Geophysics, MS-126, Rice University, 6100 Main Street, Houston, TX 77005, USA (e-mail: morganj@rice.edu; phone: 011-713-348-6330; fax: 011-713-348 5214)

## Abstract

**Discrete element simulations have been carried out to explore micromechanics and macroscopic deformation behavior of granular shear zones. Such numerical experiments allow us to look inside deforming fault zones and identify controls on fault zone structure, mechanical strength, and rheology. To date, simulations have focused on steady-state deformation of two dimensional non-cohesive granular assemblages, but more recently include velocity-dependent and time-dependent boundary conditions and contact laws. These discrete numerical simulations have successfully captured many features and behaviors observed in natural shear zones in the field and lab. The results are summarized below.**

## Introduction

Well-developed brittle faults and shear zones often contain appreciable accumulations of gouge or breccia, consisting of disaggregated and comminuted country rock and its diagenetic products. The presence of these particulate materials plays an important role in defining the structural character and mechanical behavior of the fault. In particular, experimental studies have demonstrated transitions from velocity strengthening (stable) to velocity weakening (unstable) sliding along gouge bearing shear zones, related to changes in particle size and distribution, evolving deformational fabrics, and gouge physical properties (Marone et al., 1990[4]; Beeler et al., 1996[1]). Similar processes along natural fault zones can directly influence their seismogenic potential.

Due to the discrete nature of fault gouge, fault zone properties and processes tend to be very heterogeneous, and marked by distinct discontinuities, i.e., zones of localized slip. Such complexity is difficult to capture using typical continuum theories or numerical techniques. The distinct element method (DEM) offers a unique numerical technique to study granular shear zones, preserving the discrete character of the material, and enabling direct correlations among granular micromechanics and shear zone behavior. Over the last few years, our group has carried out DEM simulations of granular shear zones, exploring controls on deformational fabrics, shear zone strength, and frictional response.

## Previous Work

Fault gouge within brittle shear zones will undergo changes in particle size and distribution with accumulated strain. Such changes have been implicated in strain-weakening that may lead to localization and instability in such faults (Biegel et al., 1989[2]). Also, particle size distributions (PSD) measured in both field and lab suggest that granular (quartz-feldspar) gouges may evolve toward a "characteristic" power-law distributed PSD (Marone and Scholz, 1989[5]; Sammis et al., 1989[8]). DEM experiments allow us to explore the influence of PSD on deformation behavior and mechanical strength, to identify dependencies that may explain these observations.

Two-dimensional (2D) DEM shear "experiments" were conducted on assemblages of discrete, noncohesive particles; particle fracture was not allowed. Scaled shear zones, about 1 cm thick, were filled with particle assemblages and sheared to 200% strain to reach residual strength conditions. Relative abundances of four particle sizes, with radii of 500, 250, 125, and 62.5  $\mu\text{m}$ , were determined assuming power-law distributions; the two-D power law exponent,  $D$ , varied from 0.81 (mostly large particles) to 2.60 (mostly small particles); interparticle friction,  $m_i$  was 0.10, 0.50, or 0.75; normal stresses ranged from 40 to 140 MPa. This suite of experiments is described in two recent papers by Morgan (1999[6]) and Morgan and Boettcher (1999[7]). The results are summarized below.

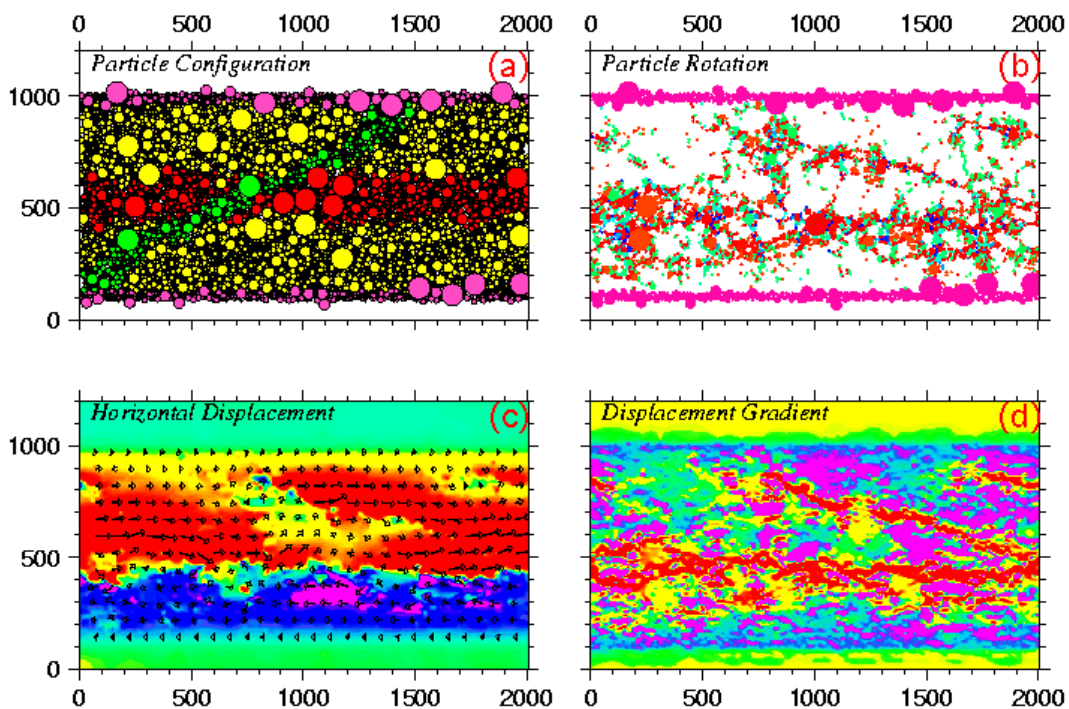


Figure 1: Snapshot of deforming assemblage,  $D = 2.60$ ,  $m_i = 0.50$ , at 140% strain (100 plotted units = 1 mm). (a) Particle configuration - gray particles in walls are fixed relative to each other; upper wall is translated to the right; colored particles within the shear zone are strain markers. (b) Particle rotations define oblique and fault parallel slip surfaces. (c) Horizontal displacements relative to homogeneous shear induced by wall displacement. (d) Gradient of horizontal displacements defines discontinuities or

slip surfaces - dark low angle and oblique slip planes represent  $Y$  and  $R_l$  surfaces respectively. (Color curves adjusted for black and white printing.)

## Deformation Structures

- Shear zone deformation was typified by formation of discrete, fault-parallel and high-angle slip planes, accommodated largely by particle rolling (Figure 1). These slip planes generally formed and dissipated within 5-10% strain.
- Simulated slip surfaces within the shear zone corresponded in orientation and sense of shear to deformation structures observed in natural and experimental gouge zones (Logan et al., 1992[3]), in particular, Reidel shears ( $R_1$ ,  $R_2$ ) and  $Y$  shears. All of the experiments showed a predominance of low-angle slip planes - typically  $Y$ -shears, which because of their shear zone parallel orientation can accommodate effectively infinite displacement. Compared to natural gouges,  $R_1$ ,  $R_2$  shears showed more extreme orientations relative to shear zone walls (~5-10° and ~85-90° respectively). However, their geometries prove to be consistent with low shear zone strength (see below).

## Particle Size Distribution

- PSD and  $m_f$  were observed to strongly influence the strength and deformation of the shear zone. Distinct changes in deformation behavior were observed, from distributed to more localized as the abundance of small particles increased (increasing  $D$  value); these were accompanied by generally decreasing shear strength. With increasing localization tendency, small particles self-organized into rows and columns of particles rolling in synthetic (consistent with shear sense) and antithetic (opposite to shear sense) directions respectively (Figure 1b).
- For simulations with  $m_f$  of 0.50, strength stabilized at  $D$  values of 1.6-2.0, PSDs similar to field and lab gouges; thus PSD controls on fault strength may preserve this "characteristic" PSD. Lower  $m_f$  experiments showed decreasing strength with  $D$ , perhaps explaining why much higher  $D$  values are observed in clay-bearing gouges.

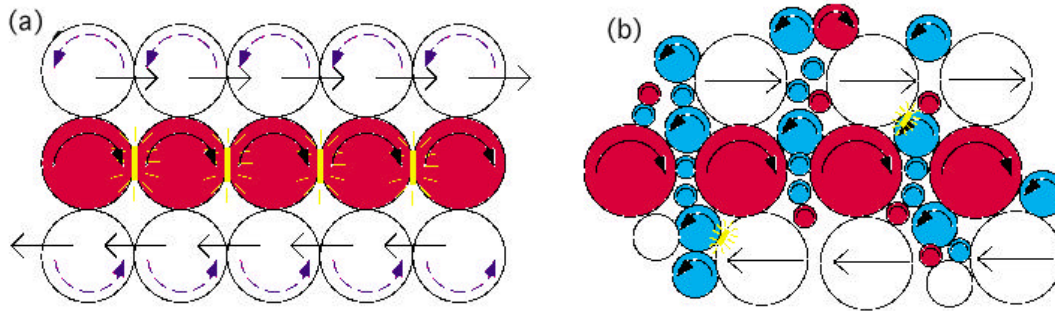
## Mechanical Behavior

- Fault friction, defined as the ratio of shear to normal stress,  $m_f = t / s_n$ , was quite low for experiments in which a constant horizontal velocity was applied to the shear zone walls.
  - Higher  $m_f$  values resulted in only slightly higher values for  $m_f$  0.25-0.32 (Figure 3). The stress-strain response of the latter experiments was similar to that of overconsolidated granular assemblages: a peak strength was reached by about 10% strain, followed by a period of strain weakening to 30-50% strain, and finally leveling out at residual strength for the rest of the test. Shear zone dilation of up to 1.5% were documented.
  - Low  $m_f$  suites yielded  $m_f$  0.20-0.25. These assemblages behaved more as normally consolidated assemblages, showing no strain weakening and minor dilation of about 0.2%.
- Shear zones with more compliant walls (simulated by a displacing spring), yielded higher shear strengths,  $m_f$  0.40-0.60, and cyclic stick-slip sliding behavior.

The low strengths of the simulated assemblages are best explained by high degrees of particle rolling. The influence on particle size distribution arises from partitioning of deformation between inter-particle sliding and rolling. Enhanced interparticle rolling occurs in assemblages with many small particles, high  $D$ , leading to self-organization of particles into rows and columns of synthetically and antithetically rotating particles (Figure 2). The high abundance of counter-rotating small particles in

moderate to high D assemblages, effectively lubricates frictional contacts between large particles, enabling shear localization, and reducing  $m_f$ . These results support the hypothesis that localization in gouge-filled shear zones results from local reductions in shear strength due to grain breakage and size reduction; however, weakening may arise from PSD controls on micromechanics rather than the kinematics of grain breakage or shear zone dilation. Although the simulations lack particle fracture, they offer insight into how micromechanics controls the mechanical evolution of granular shear zones.

Figure 2. Model for interparticle rolling in low and high D particle size distributions.



(a) Low-D (course grained) assemblages - synthetically rotating large particles slide against each other, increasing resistance, and impart counter-rotation in adjacent balls, widening shear zone; (b) high-D (finer-grained) assemblages - columns of antithetically rotating small balls "lubricate" the roller bearings. Sliding friction is restricted to low force contacts.

## Current and Future Activities

### Shear Strength, Localization and Dilation Rate

The formation of localized slip surfaces can be directly observed in the simulations. Episodes of strain localization followed sharp stress drops and were accompanied by shear zone contraction (Figure 3). Several previous studies suggested that gouge shear strength depends directly on changes in volume with strain (Marone et al., 1990[4]; Beeler et al., 1996[1]). Coupled with a dependence on sliding velocity, this leads to predictions for fault zone stability and seismogenic potential. The strength - dilation rate relationship derives from the equivalency between work performed by external stresses during shear and that dissipated by internal stresses. In a granular assemblage, the latter includes work done to overcome frictional resistance to sliding, i.e., at particle contacts, and work done to overcome normal stress on the system through dilation. This can be stated as

$$m_f = m_i + d\Delta / dg \quad (1)$$

where  $d\Delta / dg$  is the change in volume with shear strain. Here,  $m_i$  must also account for an elastic component of frictional strength, which is recovered upon unloading.

The detailed view of the shearing granular assemblage provided by these experiments allows us to test and further explore this relationship, although at this stage without velocity dependence. Shear zone friction predicted from dilation rate above, yielded a very good fit to simulated  $m_f$  - peaks and troughs matched extremely well, demonstrating that at first order these results confirm a direct

dependence of shear zone friction on dilation rate (Figure 3b). The fit to relative magnitudes of observed stress drops was not as good, suggesting additional controls on shear strength. In fact, including a negative dependence on dilation yielded an improved fit (Figure 3c). This implies that absolute assemblage volume influences shear zone strength - a reasonable interpretation, recognizing that the degree of dilation defines the number of contacts that must slide during shear.

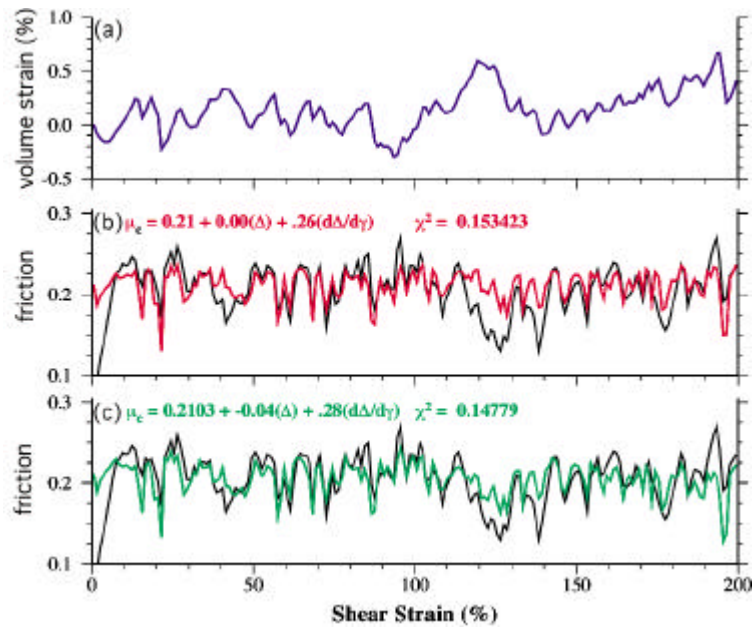


Figure 3. Relationship between volume strain and assemblage friction. (a) Volume strain (dilation) vs. shear strain. (b) Comparison of fit of equation (1) (red) to measured assemblage friction (gray). (c) Comparison of fit of equation (1) with negative dependence on volume strain (green), with assemblage friction (gray).

### Contact Laws

Although DEM simulations of granular shear zones have successfully reproduced many behaviors and geometries observed in natural and experimentally-generated shear zones, the simplified contact laws employed, specifically Hertz-Mindlin (elasto-frictional) contact laws, preclude the application of this numerical technique to complicated, realistic shear zones. In particular, shear strengths of the assemblage are consistently lower than those observed in natural materials, a phenomenon attributed to ease of particle rotation. And in the absence of evolutionary mechanisms (e.g., grain fracture, contact strengthening) that can define favorable planes of slip, shear strain is uniformly distributed over time, rather than localized into enduring zones of slip noted in natural materials.

The ability of DEM simulations to capture the macroscopic frictional behavior of real granular shear zones, such as time- and velocity-dependent sliding, depends on the use of appropriate micro-mechanical laws, e.g., for particle interactions. Intersurface rolling can be restricted as a proxy for particle angularity and out-of-plane interactions that resist rolling. As expected, these lead to higher shear strengths of the assemblage and more realistic slip plane geometries. More intriguing are consequences of time-dependent contact as has been inferred from laboratory experiments strengthening (e.g., healing; C. Marone, S. Karner, pers. comm.). Static contacts are allowed to strengthen with time, leading to increased localization of slip into zones where contacts are already

activated. The cessation of slip on that plane after stick-slip failure then requires increased shear stress to reinitiate sliding. The probability of slip now depends on relative rates of contact healing and shear strain. introducing strong velocity-dependence into the model and better capturing the macroscopic behaviors observed in laboratory experiments.

### Future opportunities

The research projects detailed above represent a sampling of possible DEM applications to the study of fault zones. The results offer intriguing insights into the micromechanics of granular friction. Our work is ultimately directed toward simulating the origin, evolution, and physical behavior of shear zones, attempting to capture and correlate realistic microscopic and macroscale properties and behaviors of these systems. Each project is a step in that direction. With enhanced computational capabilities provided by the new Center for Computational Geophysics at Rice University, we can now easily expand our simulations into 3-D, overcoming several 2-D limitations. And we continue to explore methodologies for including true velocity dependence in such simulations, as these control dynamic fault processes such as stability of fault slip and earthquake genesis.

### References

- [1] Beeler, N.M., T.E. Tullis, M.L. Blanpied, and J.D. Weeks, Frictional behavior of large displacement experimental faults, *J. Geophys. Res.*, *101*, 8697-8715, 1996.
- [2] Biegel, R.L., C.S. Sammis, and J.H. Dieterich, The frictional properties of a simulated gouge having a fractal particle distribution, *J. Struct. Geol.*, *11*, 827-846, 1989.
- [3] Logan, J.M., C.A. Dengo, N.G. Higgs, and Z.Z. Wang, Fabrics of experimental fault zones: Their development and relationship to mechanical behavior, in *Fault Mechanics and Transport Properties in Rocks*, edited by B. Evans and T.-F. Wong, pp. 33-67, Academic Press, New York, 1992.
- [4] Marone, C., C.B. Raleigh, and C.H. Scholz, Frictional behavior and constitutive modeling of simulated fault gouge, *J. Geophys. Res.*, *95*, 7007-7025, 1990.
- [5] Marone, C., and C.H. Scholz, Particle size distribution and microstructure within simulated fault gouge, *J. Struct. Geol.*, *11*, 799-814, 1989.
- [6] Morgan, J.K., 1999, Numerical simulations of granular shear zones using the distinct element method: II. The effect of particle size distribution and interparticle friction on mechanical behavior, *J. Geophys. Res. B.*, *104*, 2721-2732.
- [7] Morgan, J.K. and M.S. Boettcher, 1999, Numerical simulations of granular shear zones using the distinct element method: I. Shear zone kinematics and micromechanics of localization, *J. Geophys. Res. B.*, *104*, 2703-2719.
- [8] Sammis, C., and R. L. Biegel, Fractals, fault-gouge, and friction, *Pure Appl. Geophys.*, *131*, 256-271, 1989.

### Acknowledgments

This research was supported in part by National Science Foundation grants EAR-9805270 and EAR-0096005. Boettcher was supported by the NSF Research Experience for Undergraduates Program.